Heliyon 9 (2023) e16413

Contents lists available at ScienceDirect

Heliyon

journal homepage: www.cell.com/heliyon

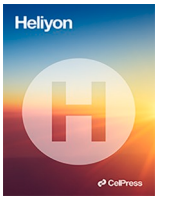

Research article

Spatial-temporal dynamics of land surface phenology over Africa for the period of 1982–2015

Siqi Shi [a,**], Peiqi Yang [b,c,*], Christiaan van der Tol [a]

[a] Faculty of Geo-Information Science and Earth Observation (ITC), University of Twente, PO Box 217, Enschede 7500 AE, the Netherlands
[b] Key Laboratory of Virtual Geographic Environment, Ministry of Education, Nanjing Normal University, Nanjing, China
[c] Jiangsu Center for Collaborative Innovation in Geographical Information Resource Development and Application, Nanjing, China

ARTICLE INFO

Keywords:
Vegetation phenology
Climate
Gradient change
Africa
Greening

ABSTRACT

Knowledge of the dynamics of vegetation phenology is essential for the understanding of vegetation-climate interactions. Although the interest in phenology study is growing, vegetation phenology in Africa received far less attention compared to the Northern Hemisphere. Africa straddles the northern and southern hemispheres, and the climate has a clear latitudinal gradient, which facilitates the study of the interaction between phenology and climate. In this study, the latitudinal and longitudinal gradients and temporal trends of start of growing season (SOS), peak of growing season (POS), and end of growing season (EOS) were examined using long-term satellite dataset during 1982–2015. The latitudinal variations in these phenology metrics were larger in the northern than those in the southern Africa, especially from 6°N northwards to 16°N. The latitudinal variations in southern Africa had no clear patterns due to the more complex climate systems. For the longitudinal variation, the temporal trends in POS and EOS exhibited a gradient-decreasing rate in northern Africa. Over the period from 1982 to 2015, the overall trends of the phenology in Africa were 'later SOS', 'later POS', and 'later EOS'. The faster rate of delay in EOS than in SOS resulted in a prolonged length of growing season (LOS) with 0.50 days/year on average in northern Africa, while a slower rate of delay in EOS than in SOS resulted in a shorter LOS with −0.12 days/year in southern Africa. The prolonged LOS in northern Africa contributes to the increase in the yearly-averaged Normalized Difference Vegetation Index (NDVI) from 1982 to 2000. Nevertheless, the NDVI appeared to have reached saturation around the 2000s, although the LOS was still extending after 2000s. Overall, the findings of this study provide an overall view of the spatial and temporal patterns of land surface phenology in the African continent, and a necessary component for future studies on the response of phenology to climate.

1. Introduction

Plant phenology is the study of periodic phenomena in plant growth and development, and how these are influenced by living environment. Periodic phenomena in plants exhibit sensitivity to decadal climate change and variability [1]. Shifts in plant phenology affect energy exchange, hydrologic cycle and carbon uptake in ecosystems, and indicate the dynamic response of terrestrial ecosystems to climate change [2]. Therefore, improved knowledge of the timing and change of phenological patterns is essential to better

* Corresponding author. Key Laboratory of Virtual Geographic Environment, Ministry of Education, Nanjing Normal University, Nanjing, China.
** Corresponding author.
E-mail addresses: s.shi@utwente.nl (S. Shi), p.yang@njnu.edu.cn (P. Yang).

https://doi.org/10.1016/j.heliyon.2023.e16413
Received 1 March 2023; Received in revised form 15 May 2023; Accepted 16 May 2023
Available online 7 June 2023

understand the interactions between the climate system and the ecological processes of ecosystems [3].

Over the past decades, the study of vegetation phenology based on ground observations and remote sensing data has gained much attention. One of the most striking patterns of phenological changes is the earlier onset of spring phenological events, i.e., the earlier start of the growing season (SOS). Advanced SOS in response to climate change has been broadly observed across Europe, North America, and Easter Asia [3,4]. Additionally, available evidence predominantly points to a delayed trend in the end of the growing season (EOS), although the magnitude is much weaker than the change in spring phenology, particularly in Northern Hemisphere (NH) [5,6,7].

Numerous studies have focused on spatial-temporal dynamics of land surface phenology (LSP) for NH, whereas the phenology study in Africa has received far less attention. Studies about phenology in Africa have reported the phenology changes with a focus on regional or country levels [8,9,10,11]. For northern Africa, the growing season generally starts between April and July. In the Sahel, Sudan, and Guinean regions in Africa, significantly delayed SOS and EOS are the main changes over the past decades [8,12]. Meanwhile, interannual and spatial variability of SOS and EOS appears highest at lower latitudes within Sudano-Sahelian West Africa [12]. In southern Africa, the growing season generally starts in October–January and ends in April-July [5,10]. In Angola, the Congo Basin, and parts of Zambia, a trend towards earlier SOS is present [13]. While delayed SOS occurs in Tanzania and Mozambique. Despite the above studies, the spatio-temporal dynamics of various phenology metrics of African vegetation are not comprehensively understood. Firstly, a complete understanding in phenological changes with long time series covering the whole African continent is still lacked. Secondly, most LSP studies to date focus on SOS/EOS/LOS, but other phenology metrics, such as the peak of growing season (POS), are less explored. POS indicates the time when the plant photosynthesis reaches its maximum value over the annual cycle [14]. The POS has the potential to characterize the productivity of terrestrial ecosystems [1] and shape the seasonality of the CO_2 concentrations in the atmosphere [15]. A study on various phenology metrics with long time series of the entire continent can provide further insight into the unique characteristics of the African terrestrial ecosystems.

Africa has a diverse range of land covers, ranging from deserts, grasslands, savannas, scrublands and woodlands to forests, including broadleaved evergreen, needleleaf evergreen and deciduous forests. The vegetation is distinct in its responses to climatic factors, resulting in great variability in phenological patterns [16]. The latitudinal variations in the phenology metrics are the strongest in the Sahel, where the regional gradients in climate and vegetation are the largest. According to the 2014 IPCC report [17], the temperature in Africa has been rising, and warming is expected to continue, although it is slightly less than that of the global land area in recent years. Spatially, these variations in climate have a clear gradient in latitude, and they play a significant role in the vegetation

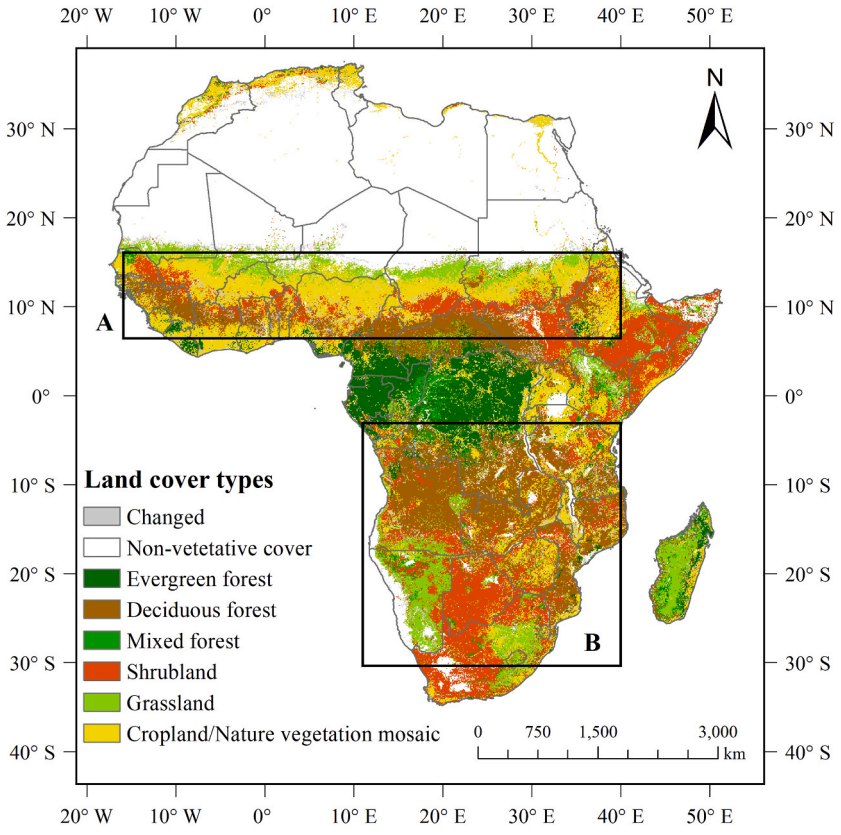

Fig. 1. Reclassified ESA CCI land cover product. The gray represented pixels where the land cover type changed during the period from 1992 to 2015. Box A is the selected region to represent northern Africa, and B for southern Africa.

dynamics on the temporal scale. Additionally, a number of recent studies report a widespread increase in greening ("re-greening") in the Sahel since the early 1980s under influence of climate change, thus re-invigorating the long-standing desertification debate [18, 19]. Some studies imply that the changes in vegetation phenology metrics (i.e. seasonal amplitude, and LOS) could be regarded as a potential factor for the "re-greening" trends [19,20]. Hence more detailed vegetation phenology information with long time series for African continent is necessary.

The overall objective of this study was to evaluate the spatial distribution and temporal trends in long time series on phenology metrics over Africa. This study focused on SOS, POS, EOS, and LOS, and explored the latitudinal and longitudinal gradients of three main phenology metrics and temporal trends in these phenology metrics over a long time series.

2. Materials and methods

2.1. Study area

The African continent spans from 37.35°N to 34.85°S, and from 17.55°W to 51.40°E, lying in both southern and northern hemispheres. Northern Africa exhibits clear regional gradients in vegetation cover, structure, and species. However, the pattern south of the equator is less clear, as regional surface features complicate climate change.

According to the annual European Space Agency Climate Change Initiative (ESA CCI) Land Cover (LC) product (https://www.esa-landcover-cci.org/), forests cover about one-fifth of the total land area of the continent, woodlands, bushlands, grasslands, and shrubland about two-fifths, and deserts and their extended margins the remaining two-fifths(Fig. 1). In northern Africa, the land cover changes from deciduous forest to grassland with increasing latitude, complying with a gradient in climate. Compared to northern Africa, the vegetation type pattern in southern Africa is more complex, including broadleaved evergreen, needleleaf evergreen, deciduous forest, shrubland, and grassland. Given the seasons spanning different calendar years and the large spatial heterogeneity of phenology in the northern and southern hemispheres, the Africa was divided into two sub-regions. To avoid bimodal areas, no-significant growing season areas, and areas often covered by clouds, this study selected these two regions as follows. The first one was located in 16°W-40°E and 6°N-16°N (marked with box A in Fig. 1), and the second one was located in 10°E − 40°E, 3°S - 30°S (box B in Fig. 1), both with rich vegetation coverages.

2.2. Data and pre-processing

The third-generation Normalized Difference Vegetation Index (NDVI3 g, version 1) dataset produced by Global Inventory Modelling and Mapping Studies (GIMMS) group (https://ecocast.arc.nasa.gov/data/pub/gimms/3g.v1/) was used to extract phenology metrics. GIMMS NDVI provides the longest time series of NDVI with reasonably high spatial and temporal resolutions. It covers a 34-year time span (1982–2015) with a spatial resolution of 8 km and a half-month interval.

Before extracting the phenology metrics, the possible snow and/or cloud pixels were removed according to the product quality flag in the NDVI product. The resulting missing values were filled with the linear interpolation approach. Subsequently, to minimize the effects of land cover type change on phenology analysis, only the pixels with the same land cover types during the period from 1992 to 2015 (according to the long-term CCI-LC product) were used in this study. Moreover, the phenology metrics could only be obtained for areas where the NDVI signal follows clearly discernible seasonal patterns, thus the non-vegetation coverage and evergreen forest were also masked out. The mean NDVI values were used to identify the non-vegetation pixels. Pixels with mean NDVI less than 0.1 were excluded. In addition to the evergreen forest marked in CCI-LC, the intra-annual variation of NDVI was also used to assist in identifying evergreen forest pixels, as a small variation is expected for those land cover. Pixels with the coefficient of intra-annual variation (CV) of the NDVI values less than 0.1 were excluded from the further analysis.

2.3. Extraction of phenology metrics

Before extracting the phenology metrics across Africa, it is necessary to consider that areas exist with bimodal growing seasons. This study first used a two-year window size to average NDVI time series (due to growing cycles in some areas can span two calendar years) to get a mean annual NDVI curve. The areas that have the following features were identified as bimodal: a) there are three or more peaks in this average NDVI curve, b) the NDVI values of the first and second largest peaks both exceed mean NDVI, c) the average of minimums should be lower than the two-year mean NDVI. These vegetated areas with bimodal or multimodal NDVI seasonality were excluded from the following analysis.

The Savitzky-Golay filtering (SG), Asymmetric Gaussian function (AG), and Double Logistic function (DL) in TIMESAT v3.3 (http://web.nateko.lu.se/timesat/timesat.asp) were employed to reconstruct NDVI time series and extract following phenology metrics: SOS, POS, EOS, and LOS. This study chose a commonly used 50% threshold to determine SOS and EOS.

$$NDVI_{ratio} = \frac{NDVI - NDVI_{min}}{Ampl} \tag{1}$$

$$\mathrm{Ampl} = NDVI_{max} - \frac{\left(NDVI_{min\_left} + NDVI_{min\_right}\right)}{2} \tag{2}$$

where the fitted NDVI values were used in the calculation instead of the raw NDVI values. $NDVI_{max}$ and $NDVI_{min}$ are maximum and minimum NDVI in each year. $NDVI_{min\_left}$ and $NDVI_{min\_right}$ are minimum NDVI from left edge and right edge. The $NDVI_{ratio}$ is defined as 50%. It means threshold of 50% of the seasonal amplitude (Ampl). The SOS is set as the day when the left edge of the growing curve increased to 50% from the left minimum. Similarly, EOS is defined as date when the right edge decreased to 50% from the right minimum. The POS is computed as the middle timing of both edges (left and right edges during a growing season) reaching the 80% level. Details of the interpretations for phenology metrics are summarized in Table 1. In TIMESAT, the 33-year phenology metrics for all pixels with single growing season were generated using three methods during 1982–2015. To minimize the error, this study ensembled the mean value of phenology metrics with these three methods.

2.4. Analysis

This study first looked at the overall trends of NDVI in Africa over the period of 1982–2015 before estimating the spatio-temporal variations of phenology metrics. The mean NDVI cycles for three decades, namely 1982–1991, 1992–2001, 2002–2010, and 2011–2015, were compared for both northern and southern Africa.

Then the phenology metrics were extracted from annual NDVI curves by long-term time series of GIMMS dataset, with a focus on spatial and temporal variations of phenology over Africa. This study was particularly interested in SOS, POS, and EOS as they can provide primary information on the shifts of vegetation phenology. Meanwhile, LOS can be calculated by the difference between EOS and SOS. The analysis was conducted in the following steps. First, this study estimated the spatial variations of each phenology metric (SOS, POS, EOS, and LOS) over Africa from 1982 to 2015. The changing latitudinal gradients of three main phenology metrics (SOS, POS, and EOS) were calculated per degree increase in latitude using Ordinary Least Squares regression (OLS). Second, temporal trends in long time series were computed as the slope of linear trends based on OLS for the temporal variations. The long-term changes of each phenology metric over time were analyzed at both pixels scales and regional scales (Region A for northern Africa and Region B for southern Africa). Last, this study investigated the gradients of three main phenological temporal trends on latitudes and longitudes. Specifically, the trends of phenology metrics were evaluated along each 5°-latitude band at latitude scales. At longitude scales, this study selected Region A as the region of interest to analyze the trends of phenology metrics along each 5°-longitude band.

3. Results

3.1. Shifting of NDVI cycles

Fig. 3 shows the comparisons of the decadal averaged NDVI cycles for 1982–1991, 1992–2001, 2002–2010, and 2011–2015 for Region A and Region B (i.e., northern and southern Africa, respectively). The details of the variations are shown in Fig. 3a and b, and these variations are summarized and illustrated in Fig. 3c and d. The shifts of NDVI cycles of vegetation in both two regions showed later POS and greater maximum NDVI values ($NDVI_{max}$) (denoted with arrows in Fig. 3a and b, and illustrated in Fig. 3c and d). In comparison, temporal changes in the first and second half of the growing season presented different changes in Region A and Region B. The changes of the NDVI cycle in Region A show for the first half of the growing season an advance over the period 1982–1992, and a delay after 1992. The second half of the growing season experienced a significant delayed shift, accompanied by a rapid decline in NDVI value (summarized in Fig. 3c and d). Compared to Region A, there is no clear shift in the first and second half of the growing season in the NDVI cycles in Region B. The slope of rising NDVI in the first half of the growing season became steeper across Region B over time. Similarly, the slope of the decline in NDVI in the second half of the growing season was also going steeper over time.

3.2. Spatial variations of phenology metrics

The mean values of phenology metrics in Africa from 1982 to 2015 derived from three methods (i.e., the SG, AG, and DL functions) are depicted in Fig. 4. The comparison of these three methods is described later. In northern Africa (Region A), all the phenology metrics showed clear gradients. The general trends were—the higher the latitude, the later SOS and POS(Fig. 4a and b), the earlier EOS (Fig. 4c), and the shorter LOS (Fig. 4d). The SOS shifted from March to July with increasing latitudes with approximately 6.94 days per degree, and POS was delayed from July to October with 2.48 days per degree of latitude increase. An opposite gradient trend occurred in EOS. It advanced from December to late October with a rate of 2.71 days/degree (Fig. 5a and Table 2). The contrasting latitudinal patterns in SOS and EOS caused an obvious gradient of decreasing LOS with latitude. In contrast, the latitudinal patterns of phenology were more complex in southern Africa (Region B). No obvious latitudinal variations in phenology metrics were observed (Fig. 5b and

Table 1
Interpretations for phenology metrics.

Phenology metrics	Definition
SOS	Time for which the left edge has increased to 50% from the left minimum level
EOS	Time for which the right edge has decreased to 50% from the right minimum level
POS	Time for the mid of the season (80% level)
LOS	Time from the start to the end of the season
NDVImax	The maximum NDVI value during a seasonality

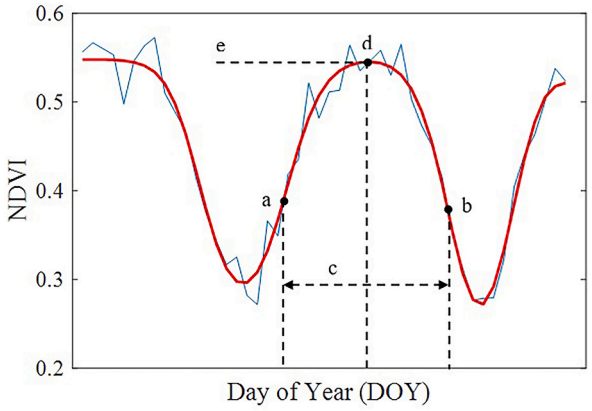

Fig. 2. Phenology metrics derived from NDVI curve: (a) SOS, (b) EOS, (c) LOS, (d) POS, (e) $NDVI_{max}$ (modified from http://web.nateko.lu.se/timesat/timesat.asp).

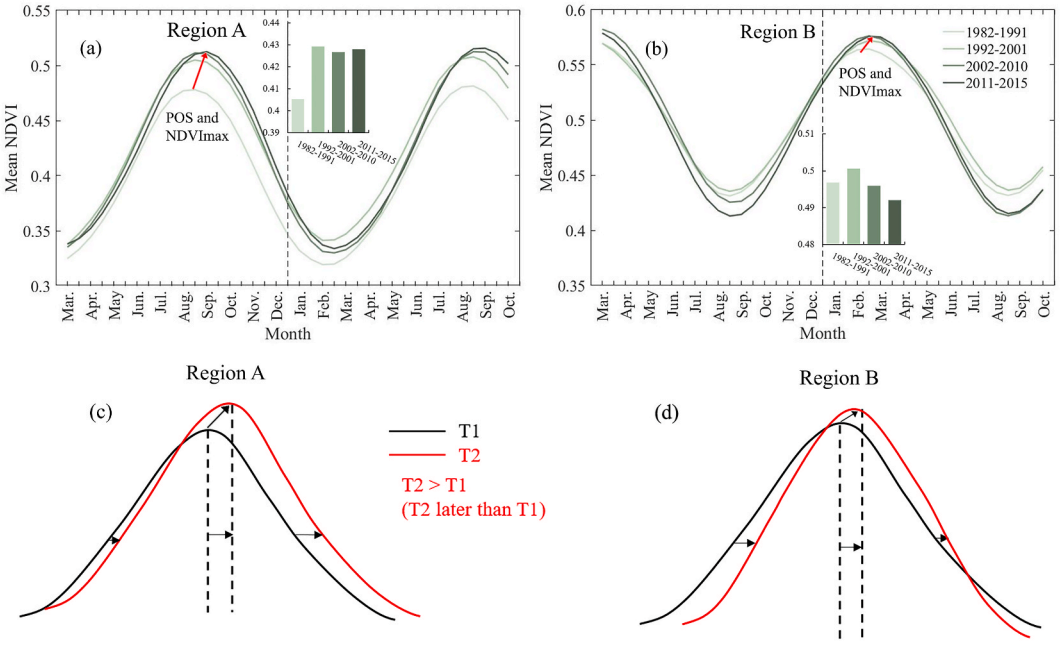

Fig. 3. Mean monthly NDVI during 1982–1991, 1992–2001, 2002–2010, and 2011–2015 averaged across regions A and B in Africa (a and b). For visual clarification, the presented NDVI values are 5-month moving averages with the x-axis indicating the center month of each window. Inset: mean annual NDVI of each period. Correspondingly, (c) and (d) present schematic diagrams of summarized growing season changes in regions A and B. T1 and T2 represent two different time sequences, "T2>T1" means T2 is later than T1.

Table 2). In this region, vegetation growth generally started between September and following January, and ended in the following year from May to August (Fig. 4a and c). POS was mainly concentrated in January–March (Fig. 4b). For the overall gradients of phenology with latitudes (Fig. 5 and Table 2), this study found that the latitudinal variations in phenology metrics begins to manifest gradually and clearly from 6° N northwards. A one degree increase would result in 11.87 and 3.54 days delayed for SOS and POS, and 3.78 days advanced for EOS, respectively.

The spatial distributions of the phenology metrics in northern and southern Africa were similar in all three methods (SG, AG, and DL function), following the variations in climates and land covers (for the spatially resolved comparison, the readers are referred to Figs. S1–S3). The results based on the three methods showed similar patterns, although there were some differences among the three filters derived key phenology metrics (SOS, POS, and EOS) at the pixel scale (Fig. S4). For example, SOS based on SG was much earlier than that based on AG and DL. AG-SOS and DL-SOS showed no remarkable difference (MEAN = −0.0262). The POS based on the three methods had minor differences, with the average differences for all pixels less than 0.4 days ($MEAN_{SG\text{-}AG}$ = −0.1427, $MEAN_{SG\text{-}DL}$ = 0.307, $MEAN_{AG\text{-}DL}$ = 0.1983). For EOS, DL-EOS was later than SG- and AG-EOS, whereas the averaged difference is within 0.2 days

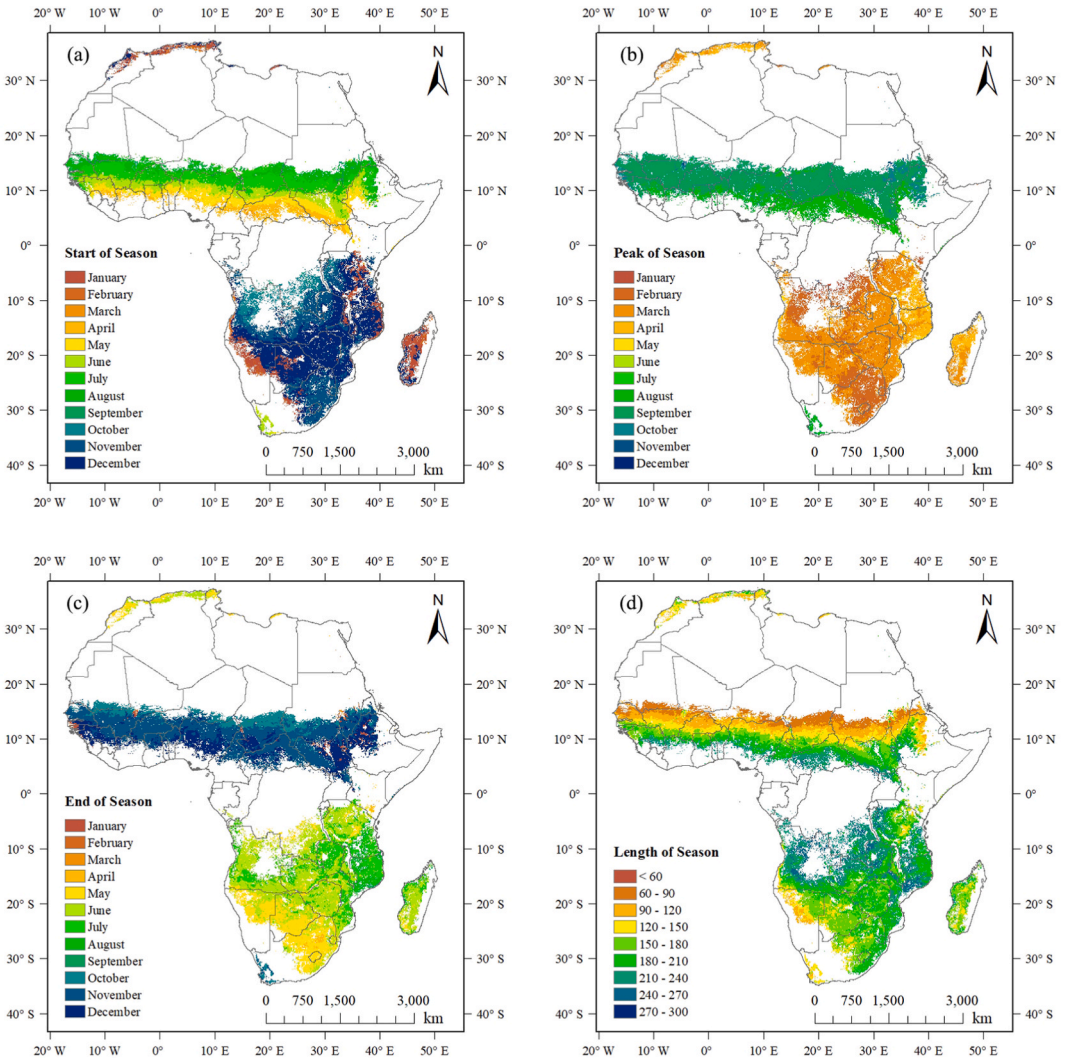

Fig. 4. The average values of phenological patterns derived from GIMMIS NDVI data. (a) start, (b)peak (c) end of season for Africa, all of them are provided in Julian day period ranges (days since January 1); (d) average length of growing season period (in days). Note that bimodal areas are marked out.

($MEAN_{SG\text{-}AG} = -0.1200$, $MEAN_{SG\text{-}DL} = -0.0371$, $MEAN_{AG\text{-}DL} = -0.1856$).

3.3. *Inter-annual variations of phenology*

Fig. 6 shows the interannual variations in phenology metrics during 1982–2015 for Regions A and B. The three main phenology metrics (SOS, POS, EOS) all presented delayed trends in both regions over time. The variations in SOS and EOS showed a delayed tendency with rates of change of 0.08 days/year for SOS and 0.58 days/year for EOS in Region A (Fig. 5a and c), and 0.24 days/year for SOS and 0.12 days/year for EOS in Region B (Fig. 5e and g). The inconsistent delayed rates of SOS and EOS resulted in different LOS changes for each region (Fig. 5d and h). The faster-delayed rate in EOS than in SOS resulted in a prolonged LOS with 0.50 days/year in Region A, while a slower rate of delayed EOS than SOS resulted in a shorter LOS with −0.12 days/year in Region B. For POS, significantly delayed trends could be observed in Region A, which were consistent with the delayed timing of peak NDVI shown in Fig. 3a. Similarly, Region B also experienced significantly delayed POS, with a rate of 0.25 days/year. This delayed trend of POS can also be observed from the NDVI cycle shifts in Fig. 3b.

More detailed spatial and temporal variations in long time series of the phenology metrics derived from GIMMS NDVI during 1982–2015 are presented in Fig. 7. It depicts large areas with significant temporal changes in SOS, POS, EOS, and LOS over the 34 years. The percentage of the area with advanced SOS was 39.3%, with only 17.3% of these pixels showing significant advance ($p < 0.05$). The areas with significantly advanced SOS include the Central African Republic and northeast Namibia (Areas marked in yellow and red, Fig. 7a). This study also observed that a part of the area (17.78% of all phenological pixels) had significantly delayed SOS,

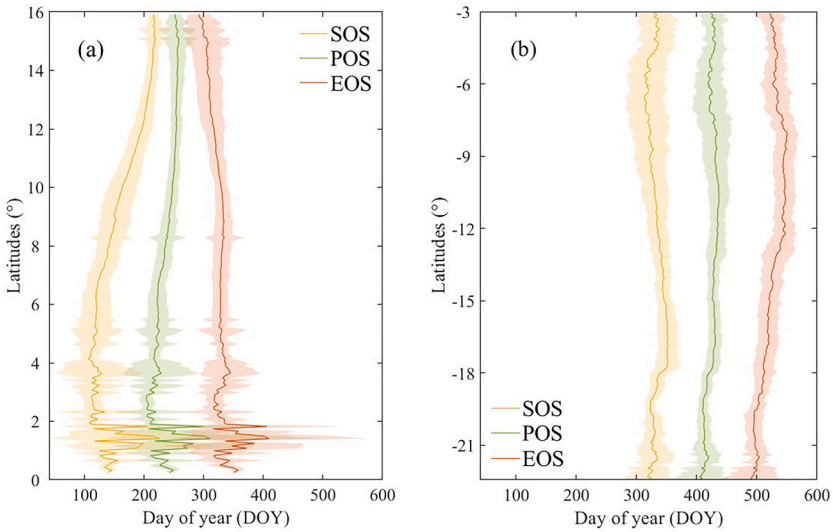

Fig. 5. Latitudinal variations in the land surface phenology, SOS, POS, and EOS for all season cycles. The shading shows the standard deviation for the average phenology on latitudinal variations.

Table 2
Dependence of phenology on Latitude in Africa, **represents $p < 0.01$

		0° - 16°N			6°N - 16°N		
		SOS	POS	EOS	SOS	POS	EOS
North	Slope(days/degree)	6.94	2.48	−2.71	11.87	3.54	−3.78
	R^2	0.63**	0.34**	0.50**	0.97**	0.83**	0.84**
		3°S - 30°S					
		SOS		POS		EOS	
South	Slope(days/degree)	0.51		−0.59		−1.75	
	R^2	0.12**		0.30**		0.59**	

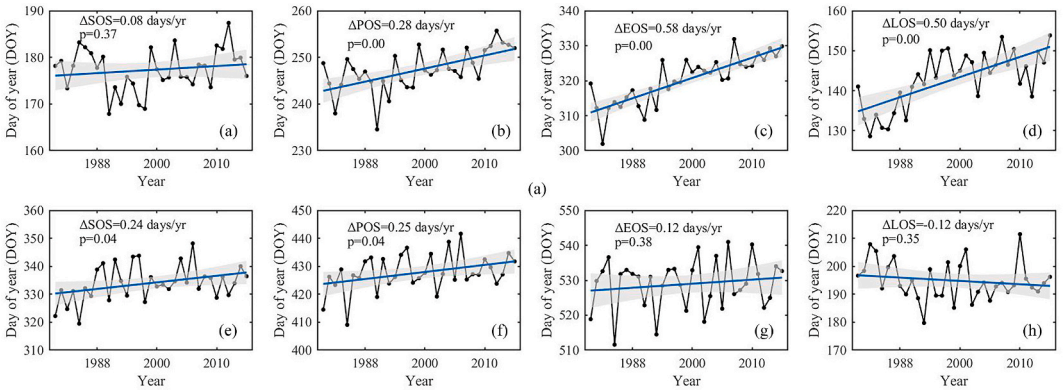

Fig. 6. Trends of phenology metrics of spatially averaged values in regions A and B (a - d for Region A, e − h for Region B), and shading area represents the 95% confidence limit of the estimated slope.

mainly located in southeast Africa, South Africa, and some parts of the Sahel (Area marked in green and blue, Fig. 7a). Almost all northern African regions had delayed EOS, while only south Angola and northeast Tanzania had significantly advanced EOS (Area marked in green and blue, Fig. 7c). Accordingly, the LOS increased for most areas in northern Africa, Northeast Namibia, the Democratic Republic of the Congo, and some of northeast Angola (Fig. 7d). However, a shortened LOS in most of southeast Africa was observed, such as in South Africa, and central Ethiopia. For POS, most areas experienced delayed dates, while only south Angola and northeast Tanzania experienced advanced POS (Fig. 7b. 30.16% for delaying and 2.81% for advancing of all phenological pixels, $p < 0.05$).

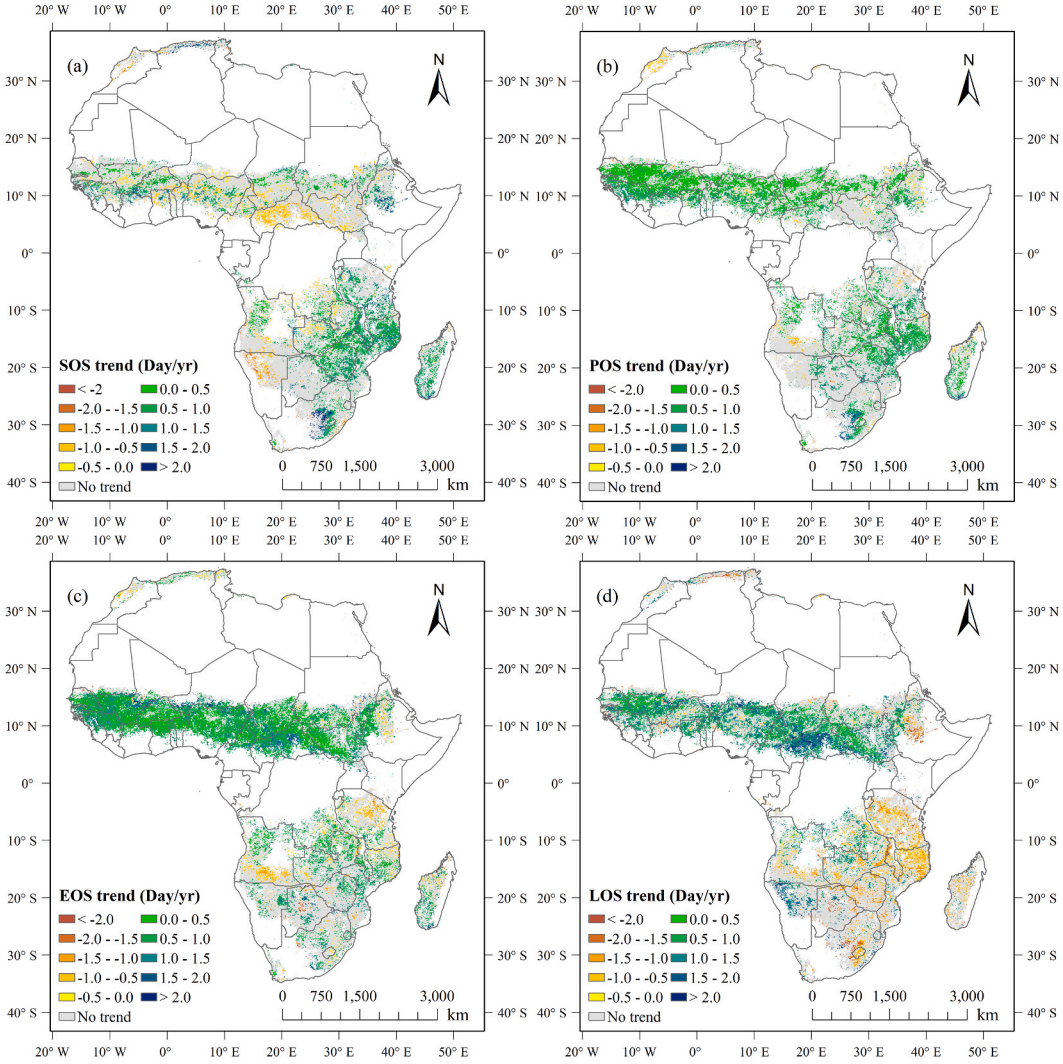

Fig. 7. The spatial distribution of the phenology metrics trends for 1982–2015 ($p < 0.05$). Gray areas represent non-significant.

3.4. Latitude- and longitude-variations in temporal trends of phenology

Further analysis of variations of temporal trends at different sub-latitudinal and sub-longitudinal zones is illustrated in Fig. 8. Table 3 also presents the gradients of phenological temporal trends with latitudes and longitudes ($d_{phenology}/d_t/d_{degree}$). For different latitudinal zones, the temporal trends of the three main phenology metrics have distinct turning points around 0° latitude. From 30°S

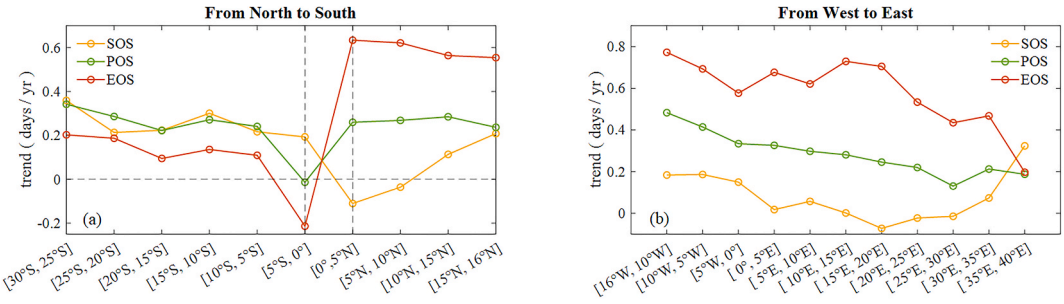

Fig. 8. Trends of phenology metrics (SOS, POS, and EOS) during 1982–2015 over different latitudinal zones (a, from the south to north) and longitudinal zones (b, from the west to east). Note that each latitudinal and longitudinal zone are averaged values of the areas of a 5° region.

to 0°, the rates of temporal trends in SOS, POS, and EOS gradually accelerated with increasing latitude ($d_{SOS}/d_t/d_{degree} = 0.004$ days/year/degree, $d_{POS}/d_t/d_{degree} = 0.011$ days/year/degree, $d_{EOS}/d_t/d_{degree} = 0.013$ days/year/degree). In contrast, the rates of temporal trends in POS and EOS decreased with increasing latitude from 0° to 16°N (−0.003 days/year/degree and −0.006 days/year/degree, respectively). The rates of temporal trend in SOS still presented positive trends along increasing latitude (Fig. 8a). The difference between the rates of temporal trends in SOS and EOS can also reveal the rate of change in LOS for different latitudinal zones. From 30°S to 0°, most latitudinal zones present faster rate of temporal trend in SOS than EOS (Fig. 8a), resulting in the shortening of LOS during 1982–2015 over southern Africa. In contrast, the rate of change in EOS was always faster than SOS from 0° to 16°N (Fig. 8a), resulting in a prolonged LOS over northern Africa. The changes of LOS could be also demonstrated in Fig. 5d.

For longitudinal zones (Region A), the temporal trends in POS and EOS exhibit a west-east gradient, with POS change rate from 0.48 days/year to 0.19 days/year and EOS change rate from 0.77 days/year to 0.20 days/year (Fig. 8b). A decrease gradient rate of temporal trend in SOS was found from west to east over 16°W-20°E, while this rate turned to increase from 20°E to 40°E. The gradually broader gap between SOS and EOS indicates the rate of change in LOS increased as longitude changes from 16°W to 20°E (Fig. 8b). Similarly, a decreased rate of change in LOS is observed from the gap between the rates of temporal trends in SOS and EOS from 20°E to 40°E (Fig. 8b).

4. Discussion

4.1. Phenology dynamics in Africa

Significant latitudinal shifts in vegetation phenology metrics throughout northern Africa were observed. The SOS was progressively delayed, while the EOS was advanced along the increasing latitudes, resulting in a shortened duration of LOS. Earlier studies reported similar gradients of SOS and EOS along latitudes [12,16,21,22]. This study also found a stronger relationship between phenology and latitude from 6° N northwards (Fig. 4). This result is similar to that reported by Zhang et al. (2005). Apart from SOS and EOS, a delayed POS from south to north was also observed, typically between July and August. From the phenological gradient in S–N direction statistically (Table 2), the latitudinal variations in POS also displayed a relatively stable change from 6° N southwards, while the latitudinal variations were more significant from 6° N northwards. Compared to northern Africa, the phenology in southern Africa was less correlated with latitude, although the three phenology metrics still exhibited significant changes statistically with increasing latitudes.

The temporal patterns of phenology may be more important to understand the vegetation activities in response to climate change. During 1982–2015, more areas experienced 'later SOS' than 'earlier SOS', while almost all areas exhibited 'later EOS' in northern Africa. Some similar trends have been individually or partly documented in other studies [8,12,23]. Due to the delayed EOS surpassing SOS in space and magnitude, a 'later and longer season' was observed in most areas. For POS, more than two-thirds of areas in northern Africa exhibited significantly delayed shifts. Compared to northern Africa, our study still provided evidence for shorter LOS, due to the faster average rate of delayed SOS than EOS in south Africa. The trend of LOS is in line with previous studies that demonstrated a shorter LOS in most areas, although the study-area ranges and periods were different [8,24,25]. Additionally, also more than two-thirds of the studied area in southern Africa experienced significantly delayed POS (Fig. 7).

4.2. Phenology dynamic associated climate drivers

The general dependence of phenology on latitude, namely the North-South discrepancy in response to latitudinal gradients is consistent with current understandings of climate systems over Africa. In northern Africa, the Intertropical Convergence Zone (ITCZ) which migrates with latitude is the dominant climate system controlling the rainy season and vegetation cycle. The ITCZ carries a water mass northward. It moves from the equator about in January to about 10°N in June in a northward direction [11]. Then in July and August, the ITCZ is at its northernmost position, approximately 15–20°N. Rainfall is received over most of the region, and the vegetation starts to grow. From September to November, the ITCZ moves southwards at a faster rate than it advanced northward earlier. The end of the rainy season tends to come suddenly, in September in the north of northern Africa and in October in the south of northern Africa [26]. In response, the vegetation reaches the end of its growing season. The corresponding phenological patterns are similar to Fig. 4 in this study. The climate system in southern Africa is more complex, including the northeasterly monsoonal flow originating from the northern inland, southeast-oriented flow from the Indian Ocean, and the westerly flow originating over the South Atlantic [27–29]. Rainfall decreases with distance from equator and a transition from bimodal to unimodal seasonal distributions. This is associated with the seasonal movement of ITCZ.

Table 3
Statistical rates of temporal trends in SOS, POS, and EOS over different latitudinal and longitudinal zones. Significant levels are coded with * ($p < 0.05$) and ** ($p < 0.01$).

	zones	Rates of temporal trends (days/year/degree)		
		SOS	POS	EOS
Latitudinal zones	0° to 30°S	0.00426	0.01066	0.01300
	0° to 16°N	0.02444**	−0.00316	−0.00592*
Longitudinal zones	16°W to 40°E	−0.00084	−0.00574**	−0.00800**

Additionally, the sea surface temperature (SST) also influences the climate and vegetation growing cycles by strongly affecting the air masses moving into the continent. In the west of southern Africa, the air masses from a subtropical high-pressure chamber over the South Atlantic are stabilized by cool Benguela current and bring little rainfall, which makes the west of southern Africa dry. However, the east of this region is wetter. The gradients of moisture (drier in the west and wetter in the east) might be linked with the west-east gradients of phenology in southern Africa (later SOS, later EOS, and longer LOS, Fig. 4). The westerly flow across the Congo Basin from the south Atlantic, southeast trades originating over the Indian Ocean bring moisture and trigger southward and northward shifts in rainfall seasonality and SOS [22,28]. As a result, the two migrations are concentrated in southern central Africa and trigger SOS shift towards southern central Africa [22]. The corresponding pattern of SOS can be observed in Fig. 4a.

Quantifying long-term changes in phenology metrics is an essential but insufficient step towards understanding the climatic drivers of vegetation dynamics. Hitherto, only few studies have assessed the relationship between phenology trends and climate change in Africa. Among these studies, the precipitation amount and rainy season time shifts were defined as a strong factor controlling the phenology changes, especially within (semi-) arid areas in most research. For instance, increased summer rain resulted in longer LOS in the central and eastern Sahel; enhanced rainfall in January and February increases the growing season by 5–15% due to enhanced southwesterly moisture transport from the tropical Atlantic [30]. However, recent studies documented pre-rain green-up phenomenon across Africa [31], which indicated a decoupling of SOS and the onset of rainy season. Other climatic or environmental cues have been proposed to trigger the phenology metrics and affect the shifts. For example, Tong et al. (2019) provided evidence for the impacts of trends in woody vegetation and fire events on phenology trends over northern and southern Africa, and [32] proposed that changes in preseason temperature might have effects on the phenology trends, as only trends in preseason temperature showed reasonable spatial overlaps while no particular spatial changes in preseason precipitation and solar radiation were found to associate with phenology trends across Africa. Although our study did not investigate the relationship between phenology trends with climate drivers, the phenology trends to climate change can be linked in existing studies. In this study, a clear gradient of slowing rates of trends in main phenology metrics (SOS, POS, and EOS) across northern Africa over different longitudinal zones was found. Huber et al. (2011) observed a similar gradient in the rate of change in rainfall, a west-east gradient of increased rainfall throughout the Sahel. This suggests that the sensitivity of phenological changes to precipitation gradually decreases with increasing rainfall, while the dominance of other factors may gradually rise. Given the complexity of climate systems in Africa, it is reasonable to consider the interannual variations in phenology are driven by a combination of multi-climate drivers. Moreover, the results of the delayed POS experienced across much of Africa highlight the importance of linking POS to climate (e.g., carbon sink) and productivity in Africa, as the POS can characterize the ability of terrestrial ecosystem productivity [15].

4.3. Linking phenology with earth greening

From interannual variations in NDVI and phenology metrics during 1982–2015, our findings suggest different NDVI changes have occurred in northern and southern Africa. Increasing averaged NDVI corresponding to increased $NDVI_{max}$ and longer LOS in northern Africa; decreasing averaged NDVI corresponding to increased $NDVI_{max}$ and shorter LOS in southern Africa. According to the mean decadal NDVI (Fig. 2), the different changes in NDVI time series were captured around the infliction point of the year 2000s. Thus, this study attempted to discuss the differences with different periods by breaking down the changes into separate decades, taking the 2000s as the turning point. The interannual variations of NDVI values were also computed for detailed analysis (Fig. S5).

Many studies have reported that Africa was turning green between 1982 and around the 2000s, especially in the Sahel, and this was largely contributed to increased rainfall [33,34]. The Sahel is composed of cropland/nature vegetation mosaic and annual grasses, and the pattern of the soil moisture strongly correlates with that of total annual rainfall [35]. During drought years, bare soil is exposed due to the absence of herbs resulting in low $NDVI_{max}$. With increased annual rainfall, annual seeds are able to germinate, fill exposed patches and cause higher $NDVI_{max}$ [8]. Our mean annual NDVI results in Fig. 2a also confirmed this finding about "greening in Sahel" during 1982–2000. However, in our findings, it should be noted that the vegetation growth or greening of northern Africa might have reached saturation around the 2000s although the LOS was still extending after 2000s (Fig. 2a and Fig. s9d). In contrast to the continuously extended LOS, the rates of $NDVI_{max}$ and Ampl increase after 2000 turned to be slight (Fig. S6), which suggests that the absolute vegetation growth in northern Africa reached a limit under continuing climate change. Another possible reason could be that greenness saturates. Because after complete land cover has been reached, vegetation biomass may still increase but this has little effect on NDVI. For southern Africa (Region B), some studies [35,36] demonstrated most areas, such as central Africa, eastern Africa, Angola, and North Botswana, presented negative trends in annual NDVI during 1982–2015. This is consistent with the decreased mean annual NDVI from 1982 to 2015 in Fig. 2b. However, the mean decadal NDVI changes suggested that greening in southern Africa exhibited an infliction point in the year 2000. Previous studies also confirmed this transformation, with a positive linear trend for mean annual NDVI before 1998, and a negative linear trend after 1998 over southeastern Africa [37]. From the outline of NDVI cycles in Fig. 2b, this study suggests that the lowered trough in NDVI cycle and substantial decline in NDVI in the second half of growing season might be the primary causes of decreased averaged NDVI since the 2000s, although the $NDVI_{max}$ and Ampl were increased over southern Africa (Fig. S6). However, from the interannual variations of NDVI, this study didn't observe the similar changes to the mean decadal variations of NDVI in southern Africa (a positive change in mean decadal NDVI before 2000s, while a negative trend after 2000s). This is most likely due to the fluctuations in the interannual NDVI variations. The fluctuations were averaged in the mean decadal NDVI. This finding highlights the importance of considering the temporal scale when analyzing earth greening in southern Africa. Overall, this result of a greening halt in Africa implies that NDVI growth changes may persist, interrupt, or reserve in the future, depending on the driving factors. This study suggest that phenology is a possible factor to explain the earth greening, while the details need to be studied further.

4.4. Limitations and prospects

Although this study provides a comprehensive study of the phenology over Africa based on GIMMS NDVI, several limitations still remain. First, the quality of GIMMS needs to be evaluated further. Due to the uniquely long satellite recording, the GIMMS NDVI dataset has been the most widely used for long-term vegetation change studies currently [38,39]. However, the GIMMS has a coarser spatial resolution (8 km) compared to other satellite datasets. Considering the Moderate Resolution Imaging Spectroradiometer (MODIS) NDVI product has higher spatial resolutions (1 km), this study used it to benchmark the quality of phenology from GIMMS NDVI. The NDVI in MOD13A2 product (Collection 6) with 1 km spatial resolution and 16-day temporal resolution from 2001 to 2015 was used. The three phenology metrics derived from GIMMS were close to MODIS overall, indicated by the close 1:1 line of the phenology metrics from these two datasets (Fig. S8a–c), although the individual differences of pixels were greater than 20 days. The differences in individual pixels might be due to different spatial (8 km of GIMMS NDVI versus originally 1 km of MOD13A2) and temporal (15-day of GIMMS NDVI versus 16-day of MOD13A2) resolution, and different sensors (GIMMS NDVI from AVHRR Sensors versus MOD13A2 from MODIS). From the interannual variations in phenology metrics derived from GIMMS and MODIS (Fig. S9), this study can observe the consistency of temporal trends in phenology between GIMMS and MODIS. Second, the bimodal areas were not analyzed in this study. An efficient algorithm for extracting phenology metrics in bimodal areas is required to be carried out in future work. Third, evergreen forest was not investigated since there is no clear seasonal cycle in NDVI. However, remote sensing Solar-induced chlorophyll Fluorescence (SIF) and Gross Primary Productivity (GPP) could be potential signals to characterize vegetation phenology for evergreen forests. Compared to reflectance-based vegetation indices (i.e. NDVI), SIF is more sensitive to the small interannual change of green biomass in the evergreen forests [40], because it can extract vegetation phenology from a physiological perspective, rather than a greenness perspective. Similarly, the change in GPP can also be an alternative approach to capture the vegetation phenology from a physiological perspective, as the shape of annual GPP is mainly affected by plant physiological activities and phenology [41]. Further progress is needed to comprehensively incorporate climate and vegetation dynamics, in combination with multi-remote sensing datasets.

5. Conclusions

Considering the insufficient understanding of the phenology over the African continent, this study provided a systemic analysis of continental-scale phenology in Africa based on the GIMMS NDVI3g product. The phenology of vegetation in northern Africa is strongly associated with the latitudes of the area—the higher latitudes, the later SOS and POS, and the earlier EOS. While in southern Africa, no apparent latitudinal variations in three key phenology metrics was observed due to the complex climate systems. Over the examined 34 years (1982–2015), the overall trends of phenology in Africa were 'later SOS and 'later EOS'. The faster-delayed rate in EOS than that in SOS resulted in prolonged LOS in northern Africa, while a weaker pace of delayed EOS than SOS resulted in shorter LOS in southern Africa. Both northern and southern Africa experienced delayed POS. Finally, longitudinal variations in temporal trends of vegetation phenology presented a west-east gradient, with slower rates of temporal trends in POS and EOS. Furthermore, the vegetation greening in northern Africa appears to have reached saturation around the 2000s, although the LOS was still extending after the 2000s. While the mean decadal NDVI in southern Africa transformed in the 2000s. The mean decadal NDVI presented a positive trend before the 2000s while a negative trend after the 2000s in southern Africa. However, the yearly-averaged NDVI did not observe this transformation. Yet, quantifying the relationships between vegetation phenology and climate or earth greening are beyond the scope of this study, which requires further investigation.

Author contribution statement

Siqi Shi: Conceived and designed the experiments, Performed the experiments, Analyzed and interpreted the data, Wrote the paper.
Peiqi Yang: Conceived and designed the experiments, Analyzed and interpreted the data, Wrote the paper.
Christiaan van der Tol: Conceived and designed the experiments, Analyzed and interpreted the data, Wrote the paper.

Data availability statement

Data will be made available on request.

Declaration of competing interest

The authors declare that they have no known competing financial interests or personal relationships that could have appeared to influence the work reported in this paper.

Acknowledgements

S. Shi was supported by the China Scholarship Council (CSC) (No. 202004910357). P. Yang was supported by the National Natural Science Foundation of China (NSFC) (No. 42101349).

Appendix A. Supplementary data

Supplementary data to this article can be found online at https://doi.org/10.1016/j.heliyon.2023.e16413.

References

[1] X. Wang, C. Wu, Estimating the peak of growing season (POS) of China's terrestrial ecosystems, Agric. For. Meteorol. 278 (2019), https://doi.org/10.1016/j.agrformet.2019.107639.
[2] A.D. Richardson, T.F. Keenan, M. Migliavacca, Y. Ryu, O. Sonnentag, M. Toomey, Climate change, phenology, and phenological control of vegetation feedbacks to the climate system, Agric. For. Meteorol. 169 (Feb. 2013) 156–173, https://doi.org/10.1016/J.AGRFORMET.2012.09.012.
[3] S. Piao, et al., Plant phenology and global climate change: current progresses and challenges, Global Change Biol. 25 (6) (2019) 1922–1940, https://doi.org/10.1111/gcb.14619.
[4] S. Ren, M. Peichl, Enhanced spatiotemporal heterogeneity and the climatic and biotic controls of autumn phenology in northern grasslands, Sep, Sci. Total Environ. 788 (2021), 147806, https://doi.org/10.1016/J.SCITOTENV.2021.147806.
[5] J.A. Caparros-Santiago, V. Rodriguez-Galiano, J. Dash, Land surface phenology as indicator of global terrestrial ecosystem dynamics: a systematic review, ISPRS J. Photogramm. Remote Sens. 171 (Jan. 2021) 330–347, https://doi.org/10.1016/J.ISPRSJPRS.2020.11.019.
[6] X. Zhang, M.A. Friedl, C.B. Schaaf, A.H. Strahler, Climate controls on vegetation phenological patterns in northern mid- and high latitudes inferred from MODIS data, Glob. Chang. Biol. 10 (7) (2004) 1133–1145, https://doi.org/10.1111/j.1529-8817.2003.00784.x.
[7] J. Jin, et al., Grassland production in response to changes in biological metrics over the Tibetan Plateau, Sci. Total Environ. 666 (May 2019) 641–651, https://doi.org/10.1016/J.SCITOTENV.2019.02.293.
[8] B.W. Heumann, J.W. Seaquist, L. Eklundh, P. Jönsson, AVHRR derived phenological change in the Sahel and Soudan, Africa, 1982-2005, Rem. Sens. Environ. 108 (4) (2007) 385–392, https://doi.org/10.1016/j.rse.2006.11.025.
[9] E.N. Chidumayo, Climate and phenology of savanna vegetation in southern africa, Jun, J. Veg. Sci. 12 (3) (2001) 347, https://doi.org/10.2307/3236848.
[10] C. Jin, X. Xiao, L. Merbold, A. Arneth, E. Veenendaal, W.L. Kutsch, Phenology and gross primary production of two dominant savanna woodland ecosystems in Southern Africa, Remote Sens. Environ. 135 (Aug. 2013) 189–201, https://doi.org/10.1016/J.RSE.2013.03.033.
[11] C. Agossou, S. Kang, Climatic factors controlling interannual variability of the onset of vegetation phenology in the northern Sub-Saharan Africa from 1988 to 2013, Afr. J. Ecol. 58 (2) (Jun. 2020) 299–308, https://doi.org/10.1111/AJE.12699.
[12] B. Butt, M.D. Turner, A. Singh, L. Brottem, Use of MODIS NDVI to evaluate changing latitudinal gradients of rangeland phenology in Sudano-Sahelian West Africa, Dec, Remote Sens. Environ. 115 (12) (2011) 3367–3376, https://doi.org/10.1016/J.RSE.2011.08.001.
[13] C.M. Ryan, M. Williams, J. Grace, E. Woollen, C.E.R. Lehmann, Pre-rain green-up is ubiquitous across southern tropical Africa: implications for temporal niche separation and model representation, New Phytol. 213 (2) (Jan. 2017) 625–633, https://doi.org/10.1111/NPH.14262.
[14] A. Gonsamo, J.M. Chen, Y.W. Ooi, Peak season plant activity shift towards spring is reflected by increasing carbon uptake by extratropical ecosystems, Glob. Chang. Biol. 24 (5) (2018) 2117–2128, https://doi.org/10.1111/gcb.14001.
[15] K. Huang, et al., Enhanced peak growth of global vegetation and its key mechanisms, Nov, Nat. Ecol. Evol. 2 (12) (2018) 1897–1905, https://doi.org/10.1038/s41559-018-0714-0.
[16] T. Adole, J. Dash, P.M. Atkinson, Characterising the land surface phenology of Africa using 500 m MODIS EVI, Appl. Geogr. 90 (Jan. 2018) 187–199, https://doi.org/10.1016/j.apgeog.2017.12.006.
[17] IPCC, *Impacts*, Adaptation, and Vulnerability: Contribution of Working Group II to the Fifth Assessment Report of the Intergovernmental Panel on Climate Change, March. 2014.
[18] A. Anyamba, C.J. Tucker, Analysis of Sahelian vegetation dynamics using NOAA-AVHRR NDVI data from 1981–2003, J. Arid Environ. 63 (3) (Nov. 2005) 596–614, https://doi.org/10.1016/J.JARIDENV.2005.03.007.
[19] L. Olsson, L. Eklundh, J. Ardö, A recent greening of the Sahel—trends, patterns and potential causes, J. Arid Environ. 63 (3) (Nov. 2005) 556–566, https://doi.org/10.1016/J.JARIDENV.2005.03.008.
[20] L. Eklundh, L. Olsson, Vegetation index trends for the African Sahel 1982–1999, Geophys. Res. Lett. 30 (8) (2003) 1430, https://doi.org/10.1029/2002GL016772.
[21] K. Guan, et al., Terrestrial hydrological controls on land surface phenology of African savannas and woodlands, J. Geophys. Res. Biogeosci. 119 (8) (2014) 1652–1669, https://doi.org/10.1002/2013JG002572.
[22] X. Zhang, M.A. Friedl, C.B. Schaaf, A.H. Strahler, Z. Liu, Monitoring the response of vegetation phenology to precipitation in Africa by coupling MODIS and TRMM instruments, Jun, J. Geophys. Res. D Atmos. 110 (12) (2005) 1–14, https://doi.org/10.1029/2004JD005263.
[23] X. Tong, F. Tian, M. Brandt, Y. Liu, W. Zhang, R. Fensholt, Trends of land surface phenology derived from passive microwave and optical remote sensing systems and associated drivers across the dry tropics 1992–2012, Oct, Remote Sens. Environ. 232 (2019) 111307, https://doi.org/10.1016/J.RSE.2019.111307.
[24] W.O. Library, B. It Sarr, B. Sarr, Present and future climate change in the semi-arid region of West Africa: a crucial input for practical adaptation in agriculture, Atmos. Sci. Lett. 13 (2) (Apr. 2012) 108–112, https://doi.org/10.1002/ASL.368.
[25] A. Vrieling, J. De Leeuw, M.Y. Said, Length of growing period over africa: variability and trends from 30 years of NDVI time series, Feb, Remote Sens. 5 (2) (2013) 982–1000, https://doi.org/10.3390/rs5020982.
[26] G. McGregor, S. Nieuwolt, Tropical Climates, Wiley, 1998.
[27] A.I. Johnson, Limnology, Climatology and Paleoclimatology of the East African Lakes, CRC Press, 1996.
[28] M.J. McHugh, J.C. Rogers, North atlantic oscillation influence on precipitation variability around the southeast african convergence zone, J. Clim. 14 (17) (2001) 3631–3642, https://doi.org/10.1175/1520-0442(2001)014<3631.
[29] K.H. Cook, The South Indian convergence zone and interannual rainfall variability over southern africa, J. Clim. 13 (21) (2000) 3789–3804, https://doi.org/10.1175/1520-0442(2000)013<3789:TSICZA>2.0.
[30] K.H. Cook, E.K. Vizy, Impact of climate change on mid-twenty-first century growing seasons in Africa, Clim. Dyn. 39 (12) (2012) 2937–2955, Nov, https://doi.org/10.1007/S00382-012-1324-1/FIGURES/13.
[31] T. Adole, J. Dash, P.M. Atkinson, Large-scale prerain vegetation green-up across Africa, Sep, Glob. Chang. Biol. 24 (9) (2018) 4054–4068, https://doi.org/10.1111/GCB.14310.
[32] T. Adole, J. Dash, V. Rodriguez-Galiano, P.M. Atkinson, Photoperiod controls vegetation phenology across Africa, Commun. Biol. 2 (1) (2019), https://doi.org/10.1038/s42003-019-0636-7.
[33] S. Huber, R. Fensholt, K. Rasmussen, Water availability as the driver of vegetation dynamics in the African Sahel from 1982 to 2007, Glob. Planet. Change 76 (3–4) (Apr. 2011) 186–195, https://doi.org/10.1016/j.gloplacha.2011.01.006.
[34] S.M. Herrmann, A. Anyamba, C.J. Tucker, Recent trends in vegetation dynamics in the African Sahel and their relationship to climate, Glob. Environ. Chang. 15 (4) (Dec. 2005) 394–404, https://doi.org/10.1016/j.gloenvcha.2005.08.004.
[35] Y. Deng, et al., Vegetation greening intensified soil drying in some semi-arid and arid areas of the world, Oct, Agric. For. Meteorol. 292–293 (2020) 108103, https://doi.org/10.1016/J.AGRFORMET.2020.108103.
[36] F. D'Adamo, B. Ogutu, M. Brandt, G. Schurgers, J. Dash, Climatic and non-climatic vegetation cover changes in the rangelands of Africa, Jul, Glob. Planet. Change 202 (2021) 103516, https://doi.org/10.1016/J.GLOPLACHA.2021.103516.

[37] W. Kalisa, et al., Assessment of climate impact on vegetation dynamics over East Africa from 1982 to 2015, 91, Sci. Rep. 9 (1) (2019) 1–20, https://doi.org/10.1038/s41598-019-53150-0. Nov.
[38] W. Ye, A.I.J.M. van Dijk, A. Huete, M. Yebra, Global trends in vegetation seasonality in the GIMMS NDVI3g and their robustness, Feb, Int. J. Appl. Earth Obs. Geoinf. 94 (2021) 102238, https://doi.org/10.1016/j.jag.2020.102238.
[39] R. Fensholt, S.R. Proud, Vegetation trends — Comparing GIMMS and MODIS global NDVI time series, Remote Sens. Environ. 119 (Apr. 2012) 131–147, https://doi.org/10.1016/J.RSE.2011.12.015.
[40] J. Zhang, et al., NIRv and SIF better estimate phenology than NDVI and EVI: effects of spring and autumn phenology on ecosystem production of planted forests, Mar, Agric. For. Meteorol. 315 (2022) 108819, https://doi.org/10.1016/J.AGRFORMET.2022.108819.
[41] S. Piao, P. Friedlingstein, P. Ciais, N. Viovy, J. Demarty, Growing season extension and its impact on terrestrial carbon cycle in the Northern Hemisphere over the past 2 decades, Sep, Global Biogeochem. Cycles 21 (3) (2007), https://doi.org/10.1029/2006GB002888.